

# Spatial and spectral superconvergence of discontinuous Galerkin method for hyperbolic problems

Emilie Marchandise<sup>a, c</sup>, Nicolas Chevaugeon<sup>a</sup>, Jean-François Remacle<sup>a, b, \*</sup>

<sup>a</sup>Department of Civil Engineering, Université Catholique de Louvain, Place du Levant 1, 1348 Louvain-la-Neuve, Belgium

<sup>b</sup>Center for Systems Engineering and Applied Mechanics (CESAME), Université Catholique de Louvain, 1348 Louvain-la-Neuve, Belgium

<sup>c</sup>Fonds National de la Recherche Scientifique, rue d'Egmont 5, 1000 Bruxelles, Belgium

Received 23 August 2005

## Abstract

In this paper, we analyze the spatial and spectral superconvergence properties of one-dimensional hyperbolic conservation law by a discontinuous Galerkin (DG) method. The analyses combine classical mathematical arguments with MATLAB experiments. Some properties of the DG schemes are discovered using discrete Fourier analyses: superconvergence of the numerical wave numbers, Radau structure of the X spatial error.

© 2007 Elsevier B.V. All rights reserved.

**Keywords:** Discontinuous Galerkin method; Superconvergence; Hyperbolic systems

## 1. Introduction

The discontinuous Galerkin method (DGM or DG method) has become a very popular numerical technique for solving hyperbolic conservation laws [5]. Some remarkable numerical properties of the DGM scheme have been demonstrated in an abundant literature. The method has been proven to be highly accurate, spectrally and spatially:

- *Spectral superconvergence:* Super-accuracy of numerical wave numbers was conjectured in [6] and subsequently proved in [2].
- *Spatial superconvergence:* Superconvergence at Radau points [4,7,1], strong superconvergence at downwind points [3] and Radau structure of the spatial error [7].

The aim of this work is to present those results in a comprehensive manner such that they become accessible to a wider community than the one of mathematicians. We propose here a unified way that allows to discover both spatial and spectral superconvergence properties of DGM's using simple MATLAB experiments. When necessary, we add to the discrete analysis some parts of mathematical proofs that highlight the discussion. In the following, we do not assume any specific choice for the numerical fluxes: upwind or not.

\* Corresponding author. Department of Civil Engineering, Université Catholique de Louvain, Place du Levant 1, 1348 Louvain-la-Neuve, Belgium.  
E-mail address: [remacle@gce.ucl.ac.be](mailto:remacle@gce.ucl.ac.be) (J.-F. Remacle).

At the end, we try to give some reasonable answers to questions that naturally come out like:

- Is it useful to apply upwind numerical fluxes, why not using centered ones?
- On a DGM scheme that use polynomial order  $p$  on a mesh of size  $h$ , the  $L^2$  norm of the error is of order  $h^{p+1}$  while the error on numerical wave numbers converges like  $h^{2p+2}$ . What is the rate of convergence to consider?
- What is the structure of the spatial error of the DGM scheme and are the jumps of the solution of any importance in the post processing (e.g. for error analysis)?

## 2. Discontinuous Galerkin space discretization in one dimension

Let us consider the following model problem. Being  $(x, t) \in (0, 1) \times (0, T)$ , find  $u(x, t)$  solution of

$$\partial_t u + c \partial_x u = 0, \quad (1)$$

with initial condition

$$u(x, 0) = u_0(x), \quad (2)$$

and periodic boundary conditions. This is a very simple model problem for an hyperbolic PDE. In (1),  $c$  is a positive number. Waves travel from left to right, in the positive  $x$  direction. We assume that time integration is exact and analyze the spatial and spectral discretization errors.

We consider a partition of the space  $(0, 1)$  in  $N$  segments of size  $\Delta x = 1/N$ . In each element, we discretize in space the unknown using Legendre polynomials of orders less or equal to  $p$ . For that, we consider a reference segment  $\xi \in (-1, 1)$  and the unknown  $u^k$  in segment  $k$  going from  $x^k = (k-1)/N$  to  $x^{k+1} = k/N$  is approximated as

$$u^k(x(\xi), t) = \sum_{i=0}^p \mathcal{P}_i(\xi) u_i^k(t), \quad \text{with } x(\xi) = x^k \frac{1-\xi}{2} + x^{k+1} \frac{1+\xi}{2}. \quad (3)$$

Fig. 1 shows the one dimensional discretization.

The Legendre polynomials we are using here have the following properties. They are orthogonal in  $(-1, 1)$  i.e. the mass matrix

$$M_{pq} = \int_{-1}^1 \mathcal{P}_p(\xi) \mathcal{P}_q(\xi) d\xi = \frac{1}{2p+1} \delta_{pq} \quad (4)$$

is diagonal.

Legendre polynomials have known values at  $\xi = \pm 1$ :

$$\mathcal{P}_p(-1) = (-1)^p \quad \text{and} \quad \mathcal{P}_p(1) = 1. \quad (5)$$

This property allows us to state that

$$u^k(x(-1), t) = \sum_{i=0}^p (-1)^i u_i^k(t) \quad \text{and} \quad u^k(x(1), t) = \sum_{i=0}^p u_i^k(t). \quad (6)$$

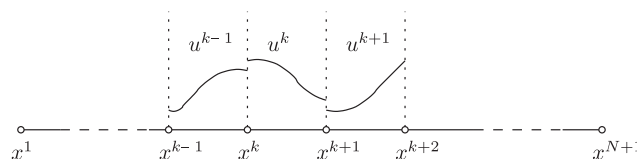


Fig. 1. One-dimensional discretization.

For our further computations, the following integral is of importance

$$D_{pq} = \int_{-1}^1 \mathcal{P}'_p \mathcal{P}_q \, d\xi.$$

First, we have that  $D_{pq} = 0$  if  $p \leq q$  because Legendre polynomial of order  $p$  is orthogonal to any polynomial of lower order and the derivative of Legendre polynomial of order  $p$  is a polynomial of order  $p - 1$ .

The other case  $p > q$  is computed using integration by parts

$$\begin{aligned} D_{pq} &= \int_{-1}^1 \mathcal{P}'_p \mathcal{P}_q \, d\xi = - \int_{-1}^1 \mathcal{P}_p \mathcal{P}'_q \, d\xi + \mathcal{P}_p \mathcal{P}_q \Big|_{-1}^1 = \underbrace{-D_{qp}}_{=0} + \mathcal{P}_p \mathcal{P}_q \Big|_{-1}^1 \\ &= 1 - (-1)^{(p+q)}. \end{aligned} \quad (7)$$

The elements of  $D_{pq}$  are then equal to 0 or 2, regardless of polynomial orders.

We construct the discontinuous Galerkin formulation  $b(u^k, v)$  of our problem, by multiplying (1) by a test function  $v(x)$ , integrating the result over a segment  $k$ , and using the divergence theorem to obtain:

$$b(u^k, v) = \int_{x^k}^{x^{k+1}} \partial_t u^k(x, t) v(x) \, dx - \int_{x^k}^{x^{k+1}} cu^k(x, t) \partial_x v(x) \, dx + [cu(x, t)v(x)]_{x=x^k}^{x=x^{k+1}} = 0 \quad \forall v. \quad (8)$$

At the interface between two elements, i.e. the end points  $x^k$  and  $x^{k+1}$ , the flux vector  $f = cu(x, t)$  is not uniquely defined and a flux formula has to be supplied to complete the discretization process. At any interface point  $x^k$ , we define the following consistent approximation of the flux

$$\bar{u}(x^k, t) = \mu u^{k-1}(x^k, t) + (1 - \mu)u^k(x^k, t), \quad (9)$$

where  $\mu$  is the upwind parameter ( $\mu = 1$  means a full upwind scheme and  $\mu = 0.5$  means a centered scheme). Eq. (8) for element  $k$  can be rewritten as:

$$\begin{aligned} b(u^k, v) &= \int_{x^k}^{x^{k+1}} \partial_t u^k(x, t) v(x) \, dx - \int_{x^k}^{x^{k+1}} cu^k(x, t) \partial_x v(x) \, dx \\ &\quad + c\bar{u}(x^{k+1}, t)v(x^{k+1}) - c\bar{u}(x^k, t)v(x^k) = 0 \quad \forall v. \end{aligned} \quad (10)$$

A second integration by parts of the second term of (10) leads to the standard *Lesaint and Raviart* [8] DG form:

$$\begin{aligned} b(u^k, v) &= \int_{x^k}^{x^{k+1}} \partial_t u^k(x, t) v(x) \, dx + \int_{x^k}^{x^{k+1}} c \partial_x u^k(x, t) v(x) \, dx + \mu c[u^k(x^k, t) - u^{k-1}(x^k, t)]v(x^k) \\ &\quad + (1 - \mu)c[u^{k+1}(x^{k+1}, t) - u^k(x^{k+1}, t)]v(x^{k+1}) = 0 \quad \forall v. \end{aligned} \quad (11)$$

Next, if we consider expansion (3) for the numerical discretization of the unknown  $u^k(x, t)$  and if we choose Legendre polynomials  $\mathcal{P}_j$  up to order  $j \leq p$  as test functions  $v(x)$ , the discrete variational formulation becomes:

$$\begin{aligned} b\left(\sum_{i=0}^p u_i^k \mathcal{P}_i, \mathcal{P}_j\right) &= \sum_{i=0}^p \left( \partial_t u_i^k(t) \Delta x \int_{-1}^1 \mathcal{P}_i \mathcal{P}_j \, dx + cu_i^k(t) \int_{-1}^1 \mathcal{P}'_i \mathcal{P}_j \, dx \right) \\ &\quad + \sum_{i=0}^p \mu c[\mathcal{P}_i(-1)u_i^k(t) - \mathcal{P}_i(1)u_i^{k-1}(t)]\mathcal{P}_j(-1) \\ &\quad + \sum_{i=0}^p (1 - \mu)c[\mathcal{P}_i(-1)u_i^{k+1}(t) - \mathcal{P}_i(1)u_i^k(t)]\mathcal{P}_j(1) = 0, \quad j = 0, \dots, p. \end{aligned} \quad (12)$$

In (12) and for  $k = 1$ , the periodic boundary condition is imposed by stating that  $u^0 = u^N$ . If we call

$$A_{ij} = (-1)^{i+j}, \quad B_{ij} = (-1)^j \quad \text{and} \quad I_{ij} = 1,$$

then (12), i.e. the discrete discontinuous Galerkin formulation on segment  $k$ , can be written in matrix form as:

$$\frac{\Delta x}{c} \partial_t u_i^k(t) M_{ij} + (D_{ij} + \mu A_{ij} - (1 - \mu) I_{ij}) u_i^k(t) - \mu B_{ij} u_i^{k-1}(t) + (1 - \mu) B_{ji} u_i^{k+1}(t) = 0. \quad (13)$$

If  $\mathbf{u}$  is a column vector of size  $N \times (p + 1)$  that contains all unknowns of every segment, the discontinuous Galerkin formulation can be written in a more compact form

$$\partial_t \mathbf{u} = -\frac{c}{\Delta x} \mathbf{M}^{-1} \mathbf{L} \mathbf{u},$$

with  $\mathbf{M} = \text{diag}(M, \dots, M)$  a block diagonal matrix whose condition number grows like  $2p + 1$  and

$$\mathbf{L} = \begin{bmatrix} (D^T + \mu A - (1 - \mu)I) & (1 - \mu)B & \cdots & -\mu B^T \\ -\mu B^T & (D^T + \mu A - (1 - \mu)I) & & \\ \vdots & & \ddots & \\ (1 - \mu)B & \cdots & -\mu B^T & (D^T + \mu A - (1 - \mu)I) \end{bmatrix},$$

a sparse matrix.

### 3. Fourier analysis

Fourier analysis consider wave-like solutions

$$u(x, t) = \text{Re}(C e^{2i\pi(kx - ft + i\sigma t)}),$$

where  $C$  is a complex constant,  $k$  is the wave number,  $f$  the frequency and  $\sigma$  is the damping parameter. The term “wave number” refers to the number of complete wave cycles that exist in one meter of linear space. Wave number  $k$  is dimensional: it is the inverse of a distance. The frequency  $f$  is dimensional too (inverse of a time). It is the number of complete wave cycles that are completed in one second.

Substituting in (1), we have the dispersion relation and no damping:

$$f = ck \quad \text{and} \quad \sigma = 0.$$

The speed of the waves is  $c$  and the solution is neither amplified nor damped. If  $\Delta x$  is the mesh size and  $k$  is the dimensional wave number, we define a non-dimensional wave number as  $k_h = k\Delta x$ . The non-dimensional wave number  $k_h$  is interpreted as a wave number where the length measure is taken as the mesh size  $\Delta x$ . For example, a non-dimensional wave number of  $k_h = \frac{1}{5}$  correspond to a wave length  $5\Delta x$  i.e. of five element sizes.

We consider the semi-discrete form of the model problem (1):

$$\partial_t \mathbf{u} + \mathbf{A} \mathbf{u} = 0, \quad \text{with} \quad \mathbf{A} = \frac{c}{\Delta x} \mathbf{M}^{-1} \mathbf{L}. \quad (14)$$

We seek how accurately the DGM scheme, i.e.  $\mathbf{A}$ , is able to approach the  $\partial_x$  operator.

It is easy to compute the spectrum of  $\mathbf{A}$  for different values of  $p$ ,  $N$  and  $\mu$  using MATLAB. We compute  $\mathbf{A}\mathbf{V} = \mathbf{V}\mathbf{D}$  where  $\mathbf{D}$  is a diagonal matrix,  $D_{ii}$  is the  $i$ th complex eigenvalue of  $\mathbf{A}$  and where the  $i$ th column of  $\mathbf{V}$  is the corresponding  $i$ th eigenvector of  $\mathbf{A}$ .

Fig. 2 shows the distribution of the discrete eigenvalues of the DGM space operator. The mesh was made of  $N = 10$  equally spaced segments. On the left Fig. 2(a), we have chosen an upwind discretization of the fluxes and in the right Fig. 2(b) a centered scheme.

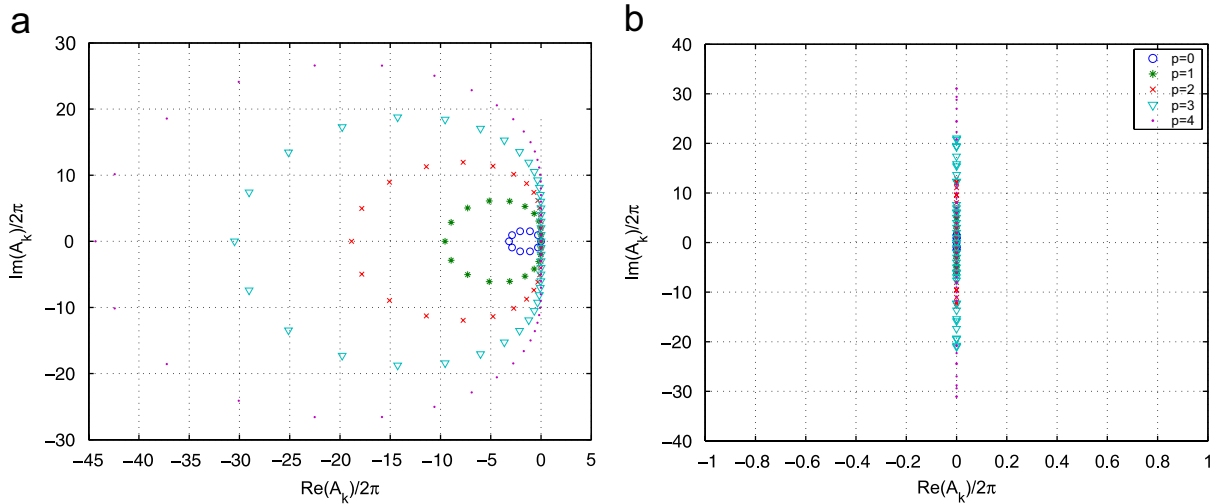


Fig. 2. Plot of the numerical eigenvalues for the DGM operator: (a) full upwind scheme ( $\mu = 1$ ); and (b) centered scheme ( $\mu = 0.5$ ).

The centered scheme seems not to produce any numerical dissipation. This can be easily shown. In order to prove the  $L^2$  stability of the DGM, we sum Eq. (11) over all elements and integrate it in time from  $t = 0$  to  $T$ :

$$\begin{aligned}
 \mathbb{B}(u^k, u^k) &= \int_0^T \sum_{k=1}^N b(u^k, u^k) dt \\
 &= \frac{1}{2} \sum_{k=1}^N \int_{x^k}^{x^{k+1}} u^k(x, T)^2 - u^k(x, 0)^2 dx - \frac{c}{2} \sum_{k=1}^N \int_0^T u^k(x^k, t)^2 - u^{k-1}(x^k, t)^2 dt \\
 &\quad + c \sum_{k=1}^N \int_0^T [\mu u^k(x^k, t) + (1 - \mu) u^{k-1}(x^k, t)] [u^k(x^k, t) - u^{k-1}(x^k, t)] dt \\
 &= \frac{1}{2} \|u(T)\|_{L^2(0,1)}^2 - \frac{1}{2} \|u(0)\|_{L^2(0,1)}^2 \\
 &\quad + c \left( \mu - \frac{1}{2} \right) \sum_{k=1}^N \int_0^T (u^k(x^k, t) - u^k(x^{k-1}, t))^2 dt = 0.
 \end{aligned} \tag{15}$$

Clearly, the scheme is  $L^2$  stable if and only if the sign of  $c$  is the same as the sign of  $\mu - \frac{1}{2}$ . Taking  $\mu = \frac{1}{2}$  leads to a scheme that exactly conserves the  $L^2$  norm of the solution (no numerical dissipation). The full upwind scheme consists in choosing  $\mu = (1 + \text{sign}(c))/2$ . In Eq. (15), we observe that the dissipation mechanism involved in the DG scheme is produced by the solution jumps.

The eigenfunction  $u_i(x)$  is constructed using the DGM interpolant:

$$u_i(x) = \text{Re} \left( \sum_{j=0}^N \mathcal{P}_j(x) V_{ji} \right).$$

The eigenfunctions  $u_i(x)$  are an approximation of the exact eigenfunctions  $U_i(x)$  of the space operator. Those can be written in the following form:

$$u_i(x) \simeq U_i(x) = \cos(2\pi k_i x + \phi_i),$$

where  $k_i$  is the wave number of the mode.

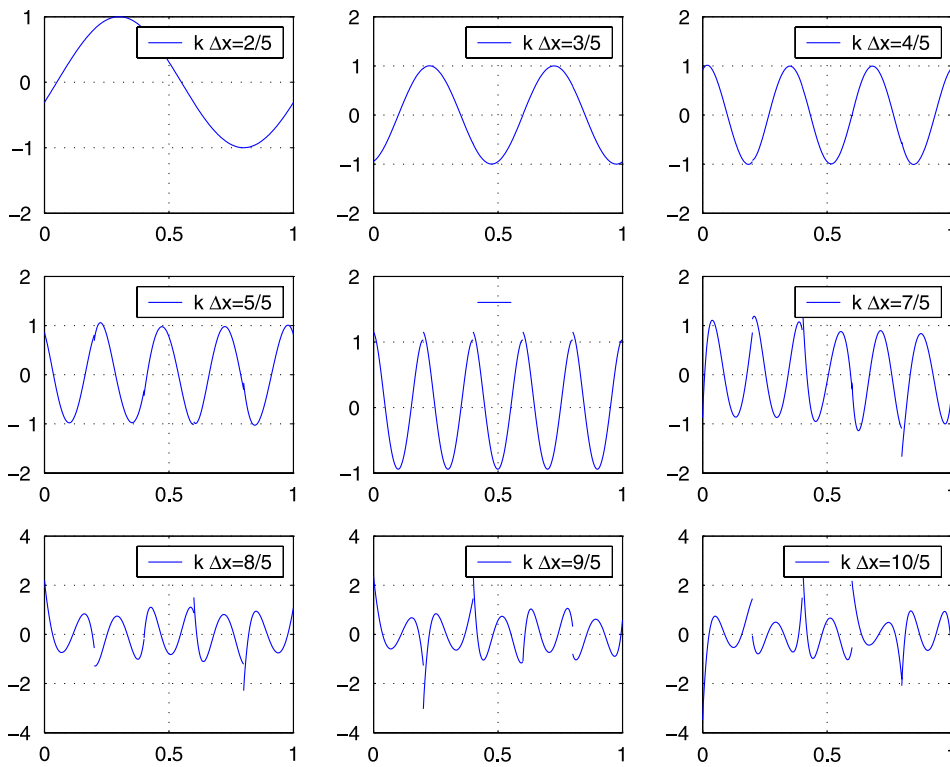


Fig. 3. Representation of nine normed eigenvectors of  $\mathbf{A}$  corresponding to different non-dimensional wave numbers  $k\Delta x$ .

In order to find the corresponding wave number  $k_i$  and the phase angle  $\phi_i$ , we first perform a fast Fourier transform (FFT) of each numerical mode  $u_i(x)$ . We use the Fourier spectrum to determine the wave number  $k_i$  of the mode: it corresponds to the maximum in the energy spectrum. The corresponding phase angle  $\phi_i$  is also given by the FFT: it is the angle of the corresponding complex Fourier coefficient.

Fig. 3 shows some of the eigenvectors of the DGM discretization. The mesh is equally spaced with  $N = 5$ ,  $p = 4$  and  $\mu = 1$ . We see that the eigenmodes corresponding to small wave numbers are well resolved, they are close to cosine functions. Higher order modes are unresolved and jumps of increasing size are appearing at inter-element boundaries. Those will be damped in time (see Eq. (15)). Actually, Ainsworth showed in [2] that the number of resolved waves grows like  $2p + 1$ . The resolved wave numbers are then such that: The resolved wave numbers corresponds to relatively small  $kh$  i.e.  $kh$  that are such that  $2p + 1 > (2\pi k\Delta x) + \mathcal{O}(k\Delta x)^{1/3}$ .<sup>1</sup> In our example, the resolved wave numbers are the ones such that  $k\Delta x < 1.43 - \mathcal{O}(kh)^{1/3}$ .

Now what happens with the non-resolved waves? We show in the next example that according to the used spatial scheme, those non-resolved waves behave differently. We advect a step function located at  $x = 0.5$  with a uniform velocity to the right without any limiter. The mesh is made of  $N = 50$  equally spaced segments. The step contains thus a very large range of wave numbers. We see in Fig. 4 that the upwind scheme dissipate the non-resolved waves while the centered scheme keep them alive. Those non-dissipated resolved waves pollute the solution. Note that the centered scheme produces spurious undamped waves that travel in the wrong direction while the upwind scheme obviously only produce waves that go from left to right. The use of an upwind scheme does not avoid the presence of oscillations. The remaining overshoots that are present at high times, when all unresolved modes are damped, correspond to resolved modes that are present in the initial solution. Those modes are going at the right speed so that they do only perturb the solution at the vicinity of the discontinuity (the solution is perfectly constant away from the discontinuity). A limiter should be able to take care of those oscillations.

<sup>1</sup> In Ainsworth's paper, wave numbers are defined differently i.e. they refer to the number of cycles in  $2\pi$  meters of linear space.

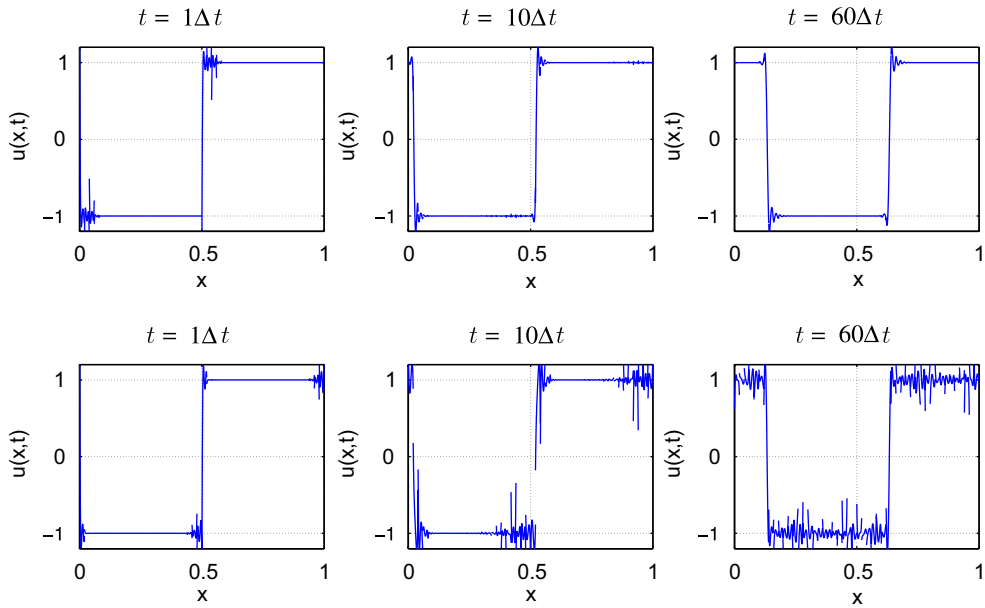


Fig. 4. Advection of a step function with upwind scheme (top) and centered scheme (bottom) ( $N = 50$ ).

We now look on how the DGM scheme is able to approximate eigenvalues and eigenfunctions of the space operator. Look at eigenfunctions will tell us about space accuracy of the DGM scheme. Looking at eigenvalues will tell us about spectral accuracy of the DGM scheme.

### 3.1. Spectral accuracy

The dispersion error usually defines how accurately the scheme is able to predict numerical wave speeds. In other words, the dispersion error of mode  $i$  is

$$E_{\text{disp}} = 2\pi k_i - \text{Im}(D_{ii}). \quad (16)$$

The dissipation error usually defines how accurately the scheme is able to predict numerical damping. The dissipation error is the error in the real part of the eigenvalues  $D_{ii}$ :

$$E_{\text{diss}} = \text{Re}(D_{ii}). \quad (17)$$

For the solution of the wave equation, the exact dissipation is null and all eigenvalues should all be on the imaginary axis.

It has been conjectured [6] and subsequently proved [2] that the numerical eigenvalues  $D_{ii}$  are superconvergent: the dispersion error is accurate to  $(kh)^{2p+3}$  and the dissipation error accurate to  $(kh)^{2p+2}$ . This means that numerical wave numbers are converging more rapidly than the actual formal accuracy of the DGM ( $\mathcal{O}(h)^{p+1}$ ). Fig. 5 illustrates the superconvergence of numerical wave numbers with  $N = 15$ ,  $p = 4$  and a full upwind scheme  $\mu = 1$ .

Note that the same kind of plots can be done for the centered case. In this case, there is no dissipation error. Dispersion errors are also superconvergent in the centered case.

### 3.2. Spatial accuracy

In this section, we look at the spatial accuracy of the DGM scheme. We look on how the scheme is able to provide an accurate approximation of the real eigenfunctions  $U_i(x)$ . We define the pointwise spatial error of mode  $i$

$$e_i(x) = u_i(x) - U_i(x).$$

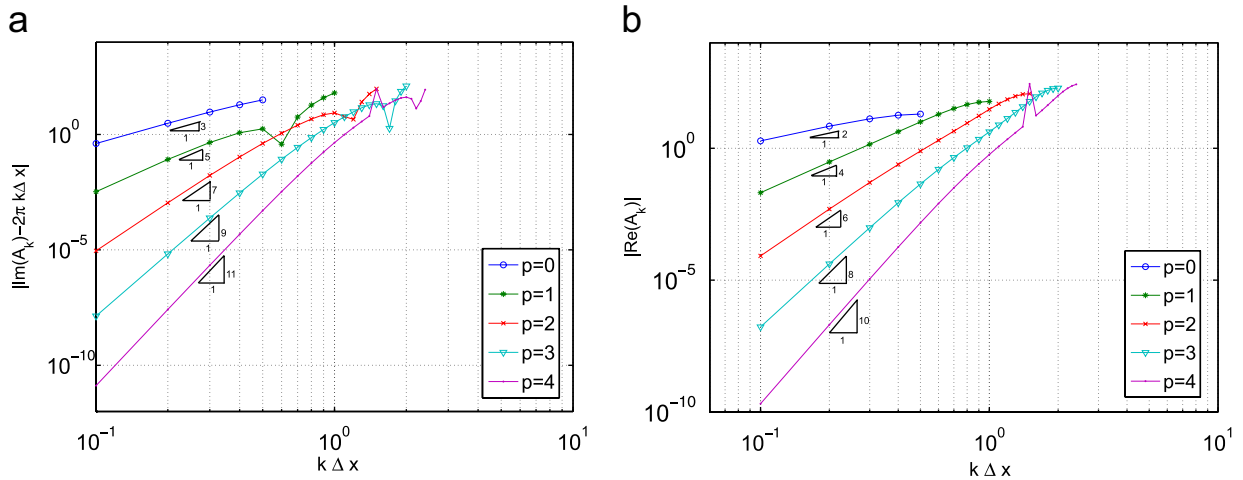


Fig. 5. Error on the numerical values of the DGM operator in the full upwind case: (a) dispersion error:  $\mathcal{O}(kh^{2p+3})$ ; and (b) dissipation error:  $\mathcal{O}(kh^{2p+2})$ .

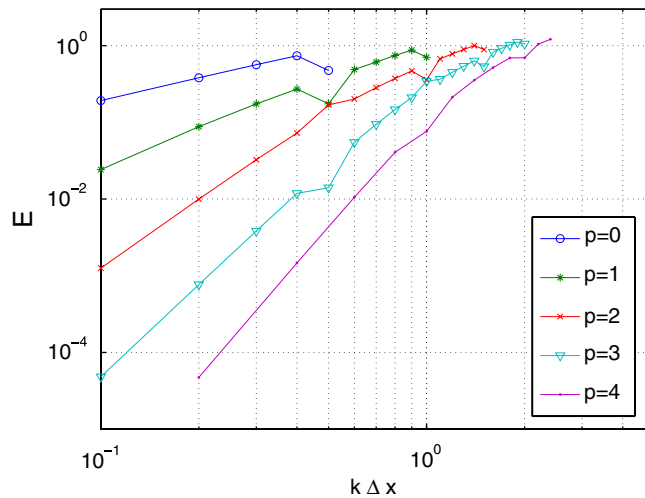


Fig. 6. Spatial error as a function of the non-dimensional wave number  $k\Delta x$ . Convergence order is  $p + 1$ .

The  $L^2$  norm of the error for mode  $i$  (wave number  $k_i$ ) is computed as

$$E_i^2 = \int_0^1 e_i^2(x) dx.$$

Fig. 6 plots spatial errors  $E$  as a function of adimensional wave numbers  $k\Delta x$ . The convergence rates are  $\mathcal{O}(k\Delta x)^{p+1}$ .

This is consistent with classical interpolation theory : approximating a function using polynomials of order  $p$  produces truncation error of order  $p + 1$ .

In Fig. 7, we plot the function  $e_i(x)$  for different  $k_i$ 's in the case  $N = 5$ ,  $p = 4$  and for two values of  $\mu$ . The existence of a structure for the DGM spatial error appears very clearly for  $\mu = 1$ : error shapes are similar for all modes and for all elements. For other values of  $\mu$ , the spatial structure disappears.



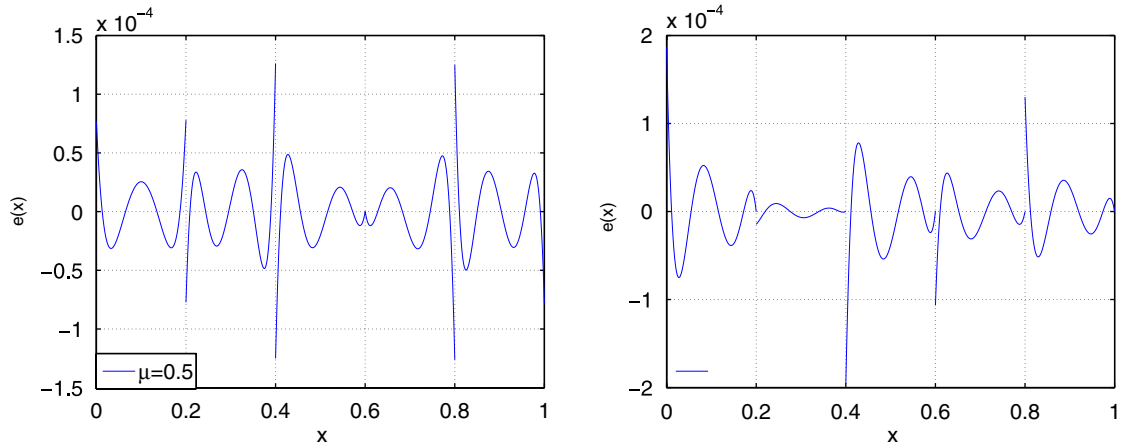


Fig. 7. Spatial error  $e(x)$  of the first eigenvectors corresponding to wave numbers  $1/\Delta x = 0.2$  for different values of  $\mu$ : (a) centered scheme ( $\mu = 0.5$ ); and (b) upwind scheme ( $\mu = 1.0$ ).

In order to find out the analytical form of the structure of the DG spatial error, we build the error functional. Taking into account that the exact solution  $u(x, t)$  is smooth, we have for one element:

$$b(U_i, \mathcal{P}_j) = \int_{x^k}^{x^{k+1}} (\partial_t U_i + c \partial_x U_i) v \, dx = 0 \quad \forall j. \quad (18)$$

Now, we assume that the solution is exact outside the element. Then, we can compute the local error functional in the upwind case. For doing so, we take the difference between Eq. (11) with  $\mu = 1$  and  $v(x) = \mathcal{P}_j$  and Eq. (18). We also assume that we have the exact solution at the downwind end, i.e.  $u_i^{k-1}(x^k) \simeq U_i(x^k)$  and get finally:

$$b(e_i^k, \mathcal{P}_j) = \int_{-1}^1 (\Delta x \partial_\xi e_i^k + c \partial_\xi e_i^k) \mathcal{P}_j \, d\xi + c e_i^k(-1, t) \mathcal{P}_j(-1) = 0 \quad \forall j. \quad (19)$$

We further assume that the leading term of the local discretization error is a polynomial of order  $p + 1$ , i.e.  $e_i^k(\xi, t) = a_{i,p+1}^k \mathcal{R}_{p+1}(\xi) + \mathcal{O}(\Delta x)^{p+2}$ . The error Eq. (19) becomes, for the leading term:

$$\int_{-1}^1 \partial_\xi \mathcal{R}_{p+1} \mathcal{P}_j \, d\xi + \mathcal{R}_{p+1} \mathcal{P}_j|_{-1} = 0 \quad \forall j. \quad (20)$$

It is easy to show, using (7), that  $\mathcal{R}_{p+1} = \mathcal{P}_{p+1} - \mathcal{P}_p$  verifies (20) and is equal to 0 at  $\xi = 1$ . Moreover, it is possible to prove [1] that the remaining terms of the error, up to  $2p$  are also Radau polynomials. For example,  $e_i(x) - a_{i,p+1}^k \mathcal{R}_{p+1} = a_{i,p+2}^k \mathcal{R}_{p+2} + \mathcal{O}(k\Delta x)^{p+3}$ . This means that the downwind points are superconvergent at order  $(k\Delta x)^{2p+1}$ .

A more general result is the following one: the flux value  $\bar{u}$  defined by Eq. (9) is always more accurate than left or right values. Let us define, respectively, the global upwind and the Riemann error for the  $i$ th eigenvector:

$$E_i^{\text{upw}} = \sum_{k=1}^N |u_i^k(x^k) - U_i(x^k)|, \quad E_i^{\text{rie}} = \sum_{k=1}^N |\bar{u}_i(x^k) - U_i(x^k)|.$$

Fig. 8 shows the behavior of these indicators with a centered and an upwind scheme. In the upwind case, downwind values ( $E_i^{\text{rie}}$ ) are superconvergent at order  $(k\Delta x)^{2p+1}$  and upwind values ( $E_i^{\text{upw}}$ ) are converging at the same rate  $(k\Delta x)^{p+1}$  as the DGM spatial error. Therefore, jumps of the solution at nodes  $u_i^k(x^k, t) - u_i^{k-1}(x^k, t)$  are a good image

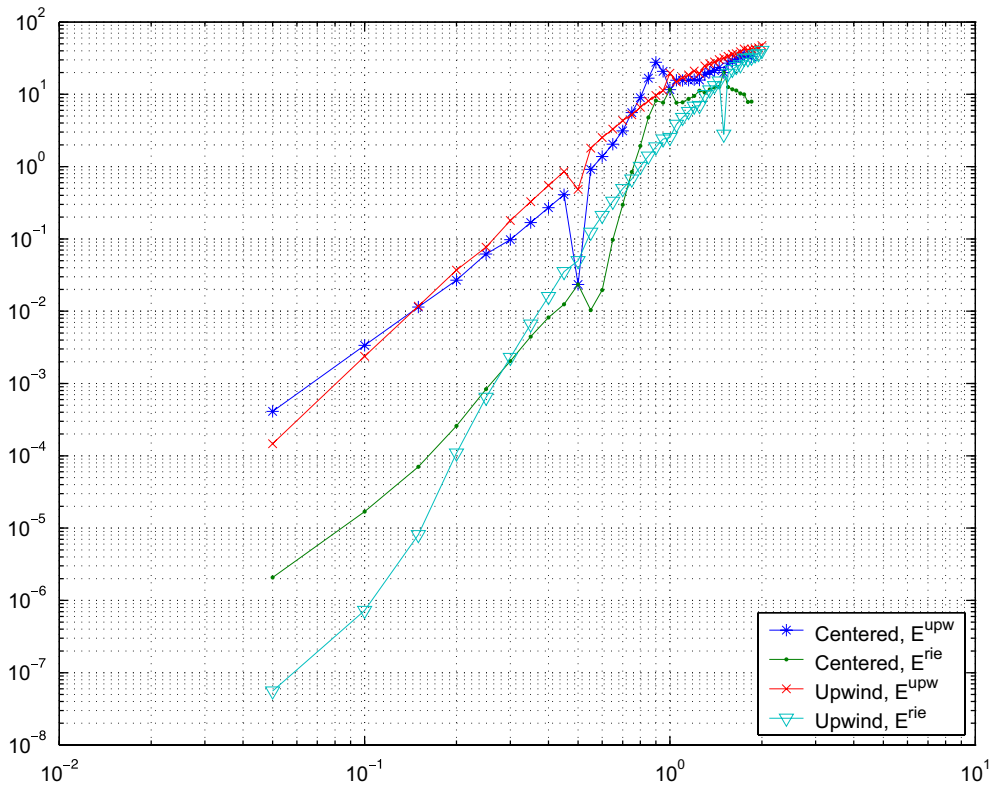


Fig. 8. Global upwind and Riemann error as a function of the non-dimensional wave number  $k\Delta x$  computed respectively with an upwind and a centered scheme.

of the local error that exists at upwind points:

$$\begin{aligned}
 J &= \sum_{k=1}^N |u_i^k(x^k) - u_i^{k-1}(x^k)| = \sum_{k=1}^N |u_i^k(x^k) - U_i(x^k) + U_i(x^k) - u_i^{k-1}(x^k)| \\
 &\leq \sum_{k=1}^N |u_i^k(x^k) - U_i(x^k)| + |u_i^{k-1}(x^k) - U_i(x^k)| \\
 &= E^{\text{upw}} + E^{\text{dwn}} = \mathcal{O}(k\Delta x)^{p+1}.
 \end{aligned}$$

In the centered case,  $E^{\text{rie}}$  is a measure of the error on solution averages at nodes. Clearly, averages are better than left or right values but are not converging better. In the centered scheme, jumps are not useful for computing local errors. This is absolutely consistent with the  $L^2$  stability result (15). In the centered case, jumps of the solution are not the cause of numerical dissipation.

#### 4. Conclusion

In this paper, we presented a simple approach to study discontinuous Galerkin schemes using simple MATLAB experiments. Both the error on numerical wave numbers and on numerical wave shapes were studied.

One of the aim of the paper was to justify the choice of the upwind scheme vs. the centered scheme. We showed that the upwind scheme was the best choice for two major reasons:

- upwind schemes allow to dissipate non-resolved modes while being super accurate on resolved ones;
- upwind schemes lead to an interesting structure of the spatial error: jumps are an image of the local discretization error.

In some further work, we will focus on the extension of the technique to 2D problems and to systems.

## References

- [1] S. Adjerid, K.D. Devine, J. Flaherty, L. Krivodonova, A posteriori error estimation for discontinuous Galerkin solutions of hyperbolic problems, *Comput. Methods Appl. Mech. Eng.* 191 (11–12) (2002) 1097–1112.
- [2] M. Ainsworth, Dispersive and dissipative behavior of high order discontinuous Galerkin finite element methods, *J. Comput. Phys.* 198 (1) (2004) 106–130.
- [3] R. Biswas, K. Devine, J. Flaherty, Parallel adaptive finite element method for conservation laws, *Appl. Numer. Math.* 14 (1984) 255–283.
- [4] B. Cockburn, E. Luskin, C.W. Shu, A. Süli, Enhanced accuracy by postprocessing for finite element methods for hyperbolic equations, in: B. Cockburn, G. Karniadakis, C.-W. Shu (Eds.), *Discontinuous Galerkin Methods, Lecture Notes in Computational Science and Engineering*, vol. 11. Springer, Berlin, 2000, pp. 291–300.
- [5] J. Flaherty, L. Krivodonova, J. Remacle, M. Shephard, Aspects of discontinuous Galerkin methods for hyperbolic conservation laws, *Finite Elem. Anal. Des.* 38 (2002) 889–908.
- [6] F. Hu, H. Atkins, Eigensolution analysis of the discontinuous Galerkin method with nonuniform grids, i, one space dimension, *J. Comput. Phys.* 182 (2) (2002) 516–545.
- [7] L. Krivodonova, J. Flaherty, Error estimation for discontinuous Galerkin solutions of two-dimensional hyperbolic problems, *Adv. Comput. Math.* 19 (1–3) (2003) 57–71.
- [8] P. Lesaint, *Sur la résolution des systèmes hyperboliques du premier ordre par la méthode des éléments finis*, Ph.D. Thesis, Université Pierre et Marie Curie, 1975.